

# Dielectric properties of epoxy/short carbon fiber composites

Z. M. Elimat · M. S. Hamideen · K. I. Schulte ·  
H. Wittich · A. de la Vega · M. Wichmann ·  
S. Buschhorn

Received: 15 February 2010/Accepted: 16 April 2010/Published online: 7 May 2010  
© Springer Science+Business Media, LLC 2010

**Abstract** The dielectric properties of epoxy/short carbon fiber composites at different concentrations 0, 5, 10 and 15% by weight, different thicknesses 2 and 4 mm, and frequency in the range from 20 Hz to 1 MHz were characterized. Scanning electron microscopy and differential scanning calorimetry were utilized. The alternating current (ac) electrical properties (complex impedance, dielectric constant, dielectric loss, real part of electric modulus, imaginary part of electric modulus, electrical conductivity, and relaxation time) were determined. It was found that the applied frequency, filler concentrations, and composite thickness affected the ac electrical properties of the epoxy/carbon fiber composites. The dielectric behaviors of the interfacial polarization between epoxy matrix and carbon fibers could be described by the Maxwell–Wagner–Sillars relaxation. The analysis of the complex electric modulus in the frequency range from 20 Hz to 1 MHz revealed that the interfacial relaxation followed the Cole–Davidson distribution of relaxation times. The universal power-law of ac conductivity was observed in the epoxy/carbon fiber composites. The calculated power exponent (near unity) is physically acceptable within this applied model.

## Introduction

Polymers have a very low concentration of free charge carriers, and thus are non-conductive and transparent to electromagnetic radiation. Thus, they are not suitable for use as enclosures for electronic equipment because they cannot shield it from outside radiation. Also they cannot prevent the escape of radiation from the component [1]. Several fillers can be added to the insulating polymeric matrix in order to achieve different conductivity ranges. Filled polymers are required for a variety of industrial applications [2, 3]. Carbon fiber/polymer composites are used in the aerospace industry on account of their high-specific stiffness and strength, which are higher than in metallic materials [4]. Conducting polymers have been extensively studied because of their potential applications in light-emitting devices, batteries, electromagnetic shielding, and other functional applications [5–7].

Carbon fibers (CFs) possess high-specific strength and specific modulus, low-expansion coefficient, and elevated thermal and electric conductivity; they are widely used in resins and in some metals as reinforcements to fabricate high-performance composites [8–11].

Epoxy resins, as organic polymer materials, have high strength, good stiffness, good thermal stability, and excellent heat, moisture, and chemical resistance. They are widely used in industrial applications in the fields of adhesives, coatings, electronics, aerospace structures, potting, composites, laminates, and encapsulation of semiconductor devices. Due to their attractive mechanical and chemical properties, epoxies are the dominant matrix material for lightweight polymer–matrix structural composites [12–15].

Many studies have been reported on the blending of epoxy with fillers [16–18]. In this work, we describe the dielectric properties of epoxy/short carbon fiber composites, measured

Z. M. Elimat (✉)  
Department of Applied Science, Ajloun University College,  
Al-Balqa' Applied University, Al-Salt, Jordan  
e-mail: ziad\_elimat@yahoo.com

M. S. Hamideen  
Department of Applied Science, Faculty of Engineering  
Technology, Al-Balqa' Applied University, Al-Salt, Jordan

K. I. Schulte · H. Wittich · A. de la Vega · M. Wichmann ·  
S. Buschhorn  
Institute of Polymers and Composites, Technische Universität  
Hamburg-Harburg, Denickestrasse 15, 21073 Hamburg,  
Germany

through the impedance technique. The alternating current (ac) electrical properties [complex impedance, real part of permittivity (dielectric constant), imaginary part of permittivity (dielectric loss), real part of electric modulus and imaginary part of electric modulus, electrical conductivity, and relaxation time] were determined.

## Experimental work

### Composite preparation

The composites were prepared in the Institute of Polymers and Composites, Technische Universität Hamburg-Harburg—Germany. The Epoxy system consisted of Araldite (LY556), an anhydride curing agent Aradur (917) and an imidazole accelerator (DY070), all provided by Huntsman, Switzerland. The short CFs (Tenax-A HT M100) with a length of ( $\leq 3 \mu\text{m}$ ) were provided by Toho Tenax Europe GmbH. The compositions (epoxy resin, CFs, hardener, and accelerator) were mixed with a mechanical stirrer for 5 min to homogenize the resulting material. It was poured into aluminum molds of ( $100 \times 180 \times 4 \text{ mm}$ ;  $100 \times 180 \times 2 \text{ mm}$ ) and cured in a programmable oven with the standard curing cycle for this particular epoxy system: 4 h at  $80^\circ\text{C}$ , followed by a postcure treatment of 8 h at  $140^\circ\text{C}$ .

### Scanning electron microscopy

The scanning electron microscope (SEM) images were taken using a Leo (Zeiss) 1530 with a field emission cathode backscatter detector and a resolution of 1 nm at 30 kV up to a  $700,000\times$  magnification choosing an accelerating voltage between 0.1 and 30 kV. For cross-section analysis, the composite samples were frozen and fractured in liquid nitrogen. All samples were coated with gold before analysis.

### Differential scanning calorimetry

The differential scanning calorimetry (DSC) thermal analysis was executed with a (NETZSCH DSC 204 F1 Phoenix<sup>®</sup>) on 10 mg of epoxy/carbon fiber composite sealed in aluminum pans. All thermograms were performed in the temperature range from 50 to  $100^\circ\text{C}$ , at a heating rate  $10^\circ\text{C}/\text{min}$ .

### Electrical measurement

Electrical measurements were performed in ac mode using an HP 4284a impedance analyzer at room temperature with voltage amplitude of 1.4 V over a frequency range from 20 Hz to 1 MHz. After curing, the samples were removed from the cavities, polished, and contacted for conductivity measurements by coating with conductive silver paint. For

electrical analysis, the samples were prepared in the form of plates having  $10 \times 10 \times 4 \text{ mm}$  dimensions.

For the dielectric analysis, the samples were placed between two parallel electrodes. A sinusoidal voltage was applied, creating an alternating electric field; this produces polarization in the samples, which oscillates at the same frequency as the electric field, but has a phase angle shift. This phase angle shift is measured by comparing the applied voltage to the measured current, which is separated into capacitive and conductive components.

### Basics

Impedance is a more general concept than resistance because it takes phase differences into account. In ac, the resistance,  $R$ , is replaced by the complex impedance,  $Z$ , which is the sum of resistance and reactance. Impedance can be written as:

$$Z = Z' + i Z'', \quad (1)$$

where  $Z'$  is the real part and  $Z''$  the imaginary part of  $Z$ . The two rectangular coordinate values are:

$$\operatorname{Re}(Z) = Z' = |Z|\cos\phi, \quad (2)$$

$$\operatorname{Im}(Z) = Z'' = |Z|\sin\phi, \quad (3)$$

with phase angle  $\phi = \tan^{-1}(Z''/Z')$  and  $|Z| = [(Z')^2 + (Z'')^2]^{1/2}$ .

The dielectric constant  $\epsilon'$  and the dielectric loss  $\epsilon''$  of the sample are calculated from the following equations:

$$\epsilon' = \frac{Z''}{2\pi f C_0 Z^2}, \quad (4)$$

$$\epsilon'' = \frac{Z'}{2\pi f C_0 Z^2}, \quad (5)$$

where  $f$  is the frequency of the applied ac electric field and  $C_0$  is the geometrical capacitance in vacuum of same dimension defined as:

$$C_0 = \epsilon_0 \frac{A}{d}, \quad (6)$$

where  $A$  is the area and  $d$  is the thickness of the sample.

The real and imaginary part of the complex electric modulus  $M^*$  was calculated from the relation:

$$M^* = M' + i M'', \quad (7)$$

where  $M'$  and  $M''$  are the real and imaginary parts of electric modulus, respectively, defined as follows:

$$M' = \epsilon' / (\epsilon'^2 + \epsilon''^2), \quad (8)$$

$$M'' = \epsilon'' / (\epsilon'^2 + \epsilon''^2), \quad (9)$$

ac electrical conductivity  $\sigma_{AC}$  has been calculated using the relation:

$$\sigma_{AC} = 2\pi f \epsilon_0 \epsilon'', \quad (10)$$

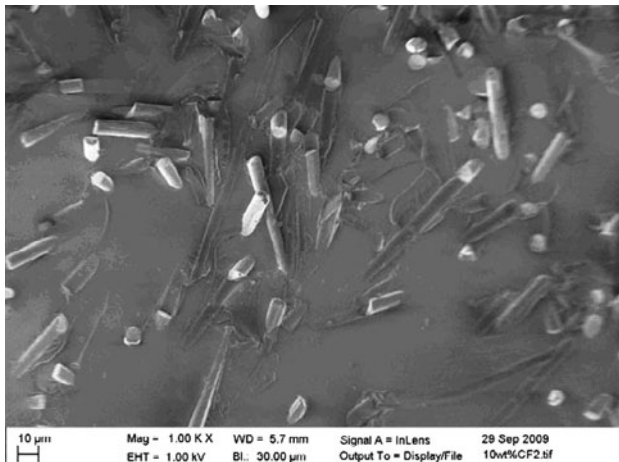
where  $f$  is the applied frequency,  $\epsilon_0$  is the permittivity of the free space, and  $\epsilon''$  is the dielectric loss.

## Results and discussions

From the SEM study, some information may be inferred about strength of fiber–matrix interactions and fiber surfaces. Extensive poor interfacial adhesion can also be observed using SEM analysis. Additionally, adhesive failure in the interface between carbon fiber and epoxy matrix can be proved by SEM analysis. Figure 1 shows the SEM micrographs of the 10 wt% short carbon fiber composites.

The glass transition temperatures of the composites can be determined based on the DSC results. The endothermic step transition located at the 140–150 °C temperature range; the glass transition temperatures values are shown in Table 1.

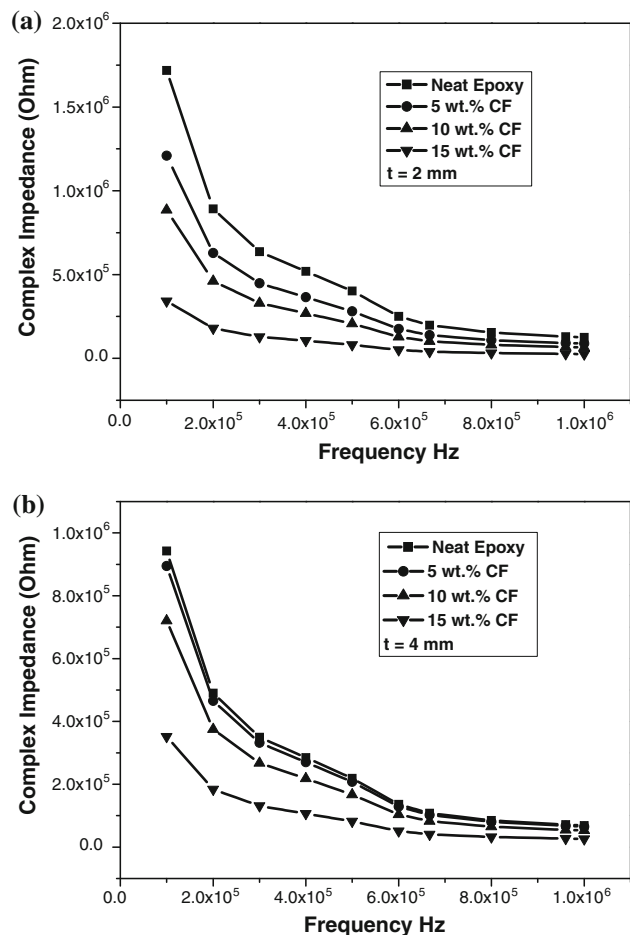
Figure 2a and b represents the dependence of the complex impedance on the frequency for epoxy/short carbon fiber composites. The figure show that the impedance decreases with increasing frequency, the carbon fiber concentration, and sample thickness. The decrease in



**Fig. 1** The SEM micrographs of the 10 wt% short carbon fiber composites

**Table 1**  $T_g$ ,  $A$ , and  $n$  values for composites with different thicknesses

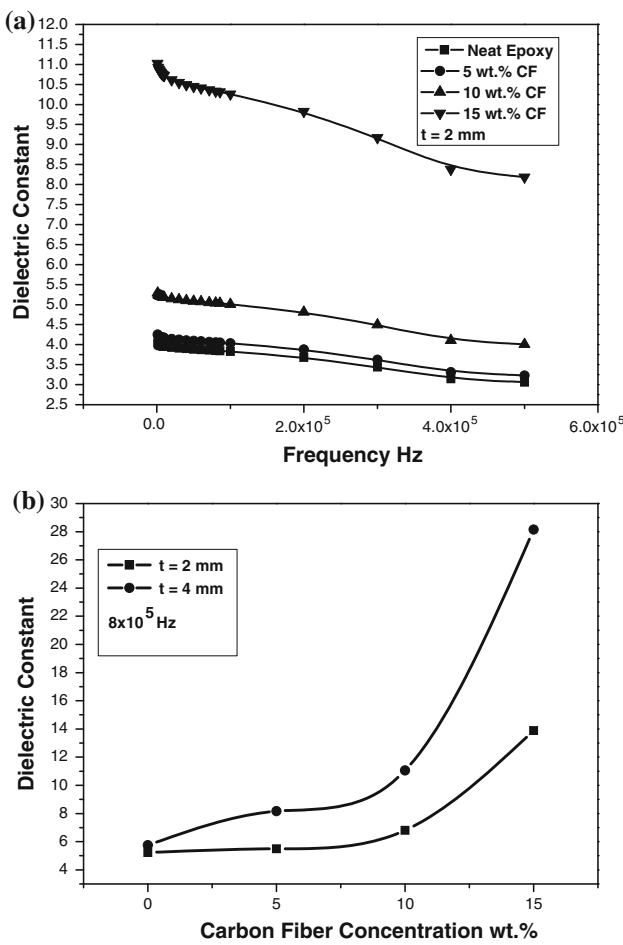
Composite	$T_g$ (°C)	$t = 2$ mm		$t = 4$ mm	
		$n$	$A$	$n$	$A$
Neat epoxy	147.7	1.17	4.83E-6	1.30	2.65E-6
5 wt% CF	145.4	1.16	4.78E-6	1.20	4.88E-6
10 wt% CF	146.4	1.13	6.58E-6	1.17	7.06E-6
15 wt% CF	147.0	1.05	1.49E-5	0.85	6.90E-5



**Fig. 2** The dependence of the complex impedance on the frequency for epoxy/short carbon fiber composites

impedance indicates that the material becomes more conductive. This behavior may be attributed to the increase in the fiber to fiber contacts of carbon fiber paths in the epoxy matrix [19–21].

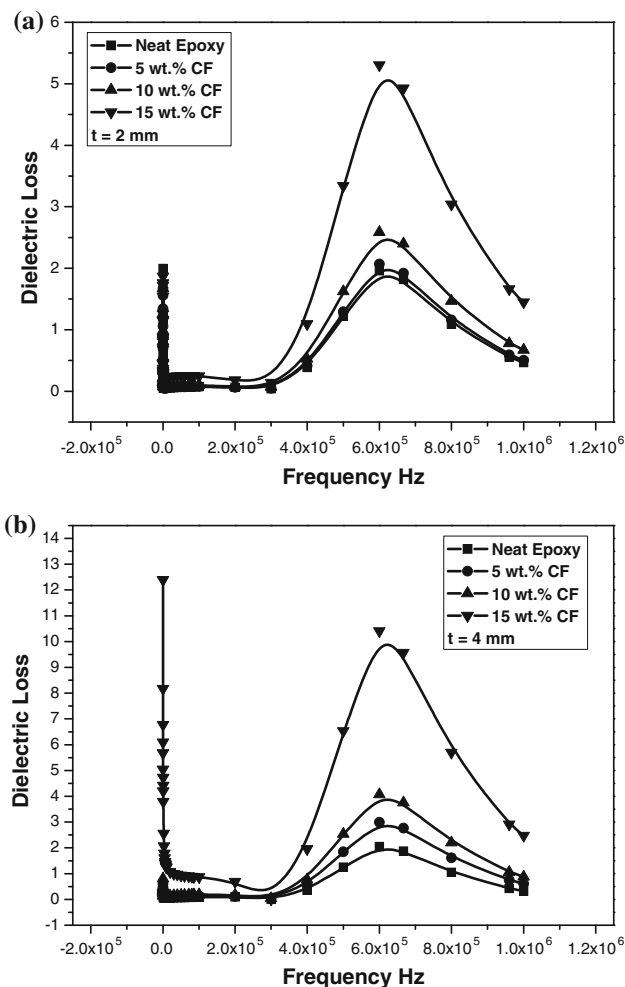
From Fig. 3a and b, it is clear that the values of dielectric constant, given for an epoxy resin loaded with CFs at different concentrations, increased with increasing the carbon fiber content. This result can be attributed to the increase in the polarity of all blends due to the increase of carbon fiber concentration, which in turn leads to an increase in the orientation polarization and also to the presence of interfacial polarization [22]. The increment in permittivity with the decrease of frequency reveals that the system exhibits the interfacial polarization at low frequency. As reported by Soares et al. [22], the strong low-frequency dispersion for  $\epsilon'$  and no loss peak for  $\epsilon''$ , as shown in Fig. 4a and b, are characteristics of charged carrier systems. It is also clear that the curves relating dielectric loss, as shown in Fig. 5a and b, are broader than the Debye curve indicating the presence of more than one relaxation process. These processes can be attributed to



**Fig. 3** The dependence of the dielectric constant on the frequency for epoxy/short carbon fiber composites

relaxation mechanisms related to the main chain and its related motions [23]. One of the expected mechanisms is related to the interfacial polarization, which usually occurs at the lower frequency range for heterogeneous systems. The origin of such a process is an ac current that is in phase with the applied potential due to the difference in permittivities and resistivities of the blends [24].

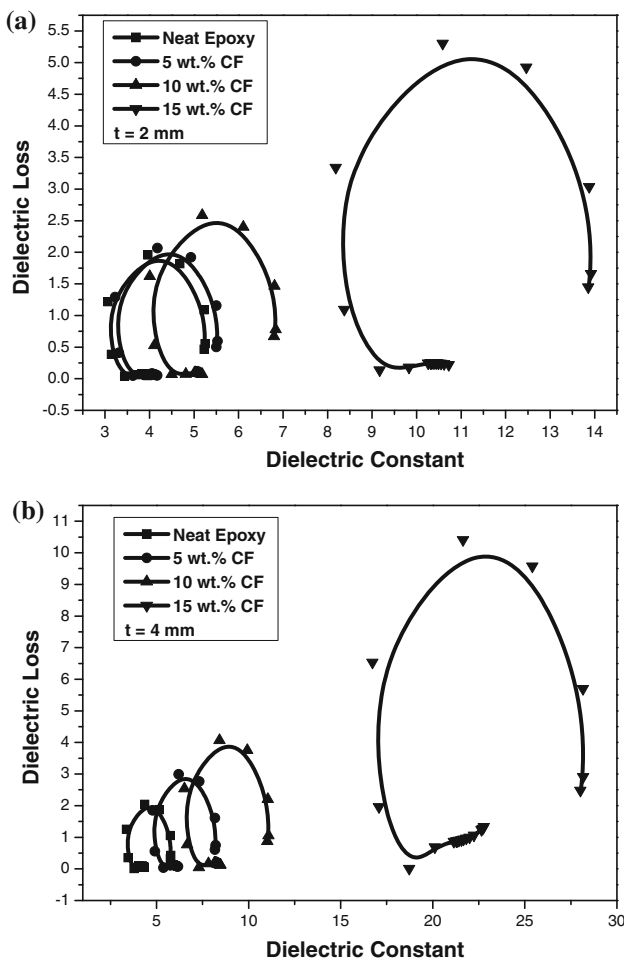
On transforming the dielectric permittivity and loss values into the electric modulus formalism, obtained in Fig. 6a and b, gives the real part  $M'$  and the imaginary part  $M''$  of the electric modulus versus frequency for the epoxy matrix. It can be clearly seen that values of  $M'$  increased with frequency at a constant temperature and reached a rather constant value at the end of the spectrum. The evolution toward a constant value of  $M'$  at high frequency is due to the fact that polarization is ineffective at high frequency, since the dipoles cannot follow the applied electric field when the frequency is very high. The variation of the imaginary part of the electric modulus according to the temperature of the epoxy is given in Fig. 7a and b. We note the presence of two relaxation peaks related to



**Fig. 4** The dependence of the dielectric loss on the frequency for epoxy/short carbon fiber composites

ionic conduction at low frequency and a relaxation associated with the glass transition for the high frequencies. These two relaxation peaks shifted to high temperature when the frequency increased [25–28].

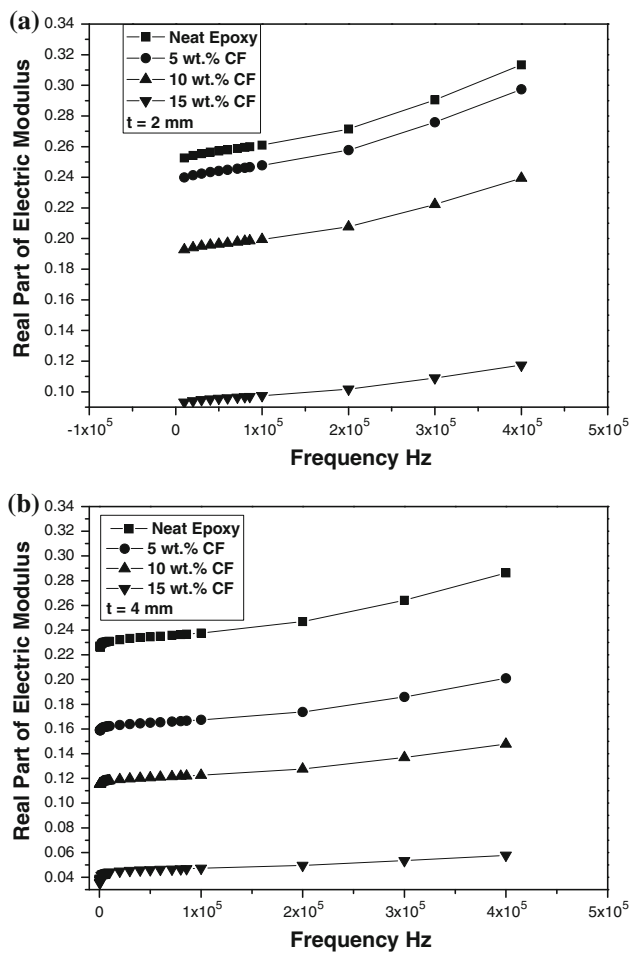
The complex plane diagram of the electric modulus, illustrated in Fig. 8a and b, displays single arcs, which prove the existence of the interfacial or the Maxwell–Wagner–Sillars (MWS) relaxation process. Furthermore, it can be regarded as the transition from resistive conduction through the conduction networks of CFs (namely, through the  $R_c$ ) to the capacitance conduction through the capacitors (namely, through the  $C_c$ ) in the matrix. The suppressed semi-circles in the Cole–Cole diagram correspond to the relaxation processes for each of the specimens. Generally, in systems with a conductive component, interfacial relaxation is obscured by conductivity and the dielectric permittivity may be high at low frequencies. To overcome this difficulty in evaluating interfacial polarization, it has been decided to use the electric modulus formalism. It has also



**Fig. 5** Debye curves

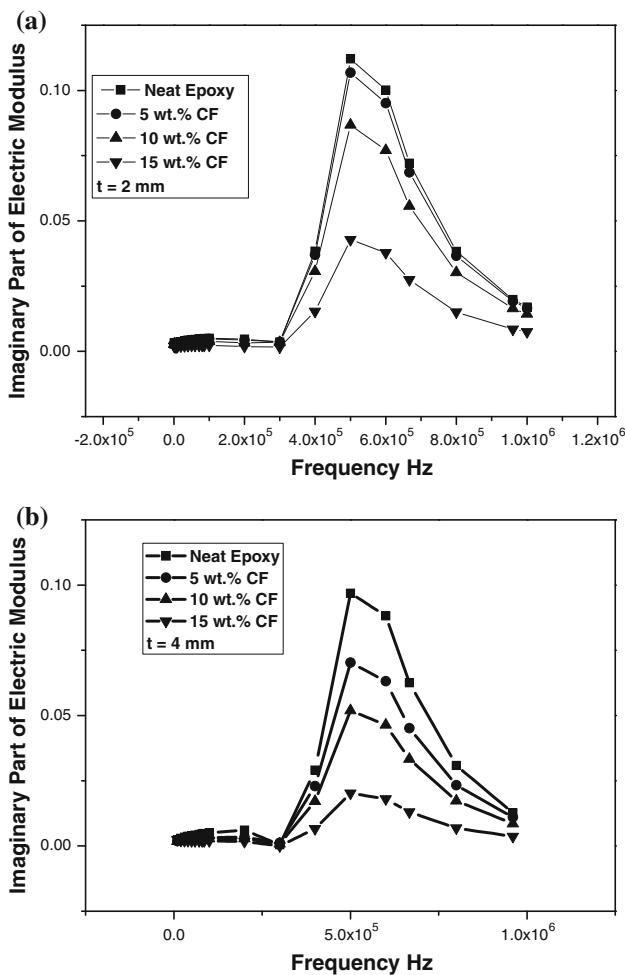
been used to study the conductivity relaxation behaviors of polymers. An advantage of adopting the electric modulus to interpret bulk relaxation properties is that variations in the large values of permittivity and conductivity at low frequencies are minimized. In this way, the familiar difficulties caused by electrode nature and contact, space charge injection phenomena, and absorbed impurity conduction effects, which appear to obscure relaxation in the permittivity presentation, can be resolved or ignored [17]. The shift of  $M'$  and  $M''$  to higher frequency with the increasing heat treatment time provides the experimental evidence of dynamic percolation. This shifting also indicates that the resistance, which is the sum of the small resistors made of carbon fillers in the matrix, becomes more significant than capacitance conductivity attributed to capacitors made of the gaps between CFs [25–27].

Figure 9a and b shows the variation of the ac electrical conductivity with the filler concentrations at different frequency. The conductivity in all compositions increases with the frequency applied. This increase means charge carriers are sufficiently free to follow the changing electric



**Fig. 6** The real part ( $M'$ ) of the electric modulus versus the applied frequency for epoxy/short carbon fiber composites

field and, therefore, conductivity is frequency dependent. At higher frequencies, the conductivity increases rapidly indicating a breakdown of the dielectric. When the concentration of CFs is high enough, a continuous carbon network is formed in the solid polymer matrix. As we know, the electron tunneling is a dominant transport process in carbon fiber–polymer composites, and the electrical conductance depends on the distance between neighboring CFs. Hence, the composites can be regarded as the system composed of random arrays of closely spaced conductors, dispersed in an insulating polymer matrix. The degree of the contacts of the fibers may be varied according to the dispersion mode of the CFs and the morphology of the polymer matrix. At low frequencies, we observed that the conductivity depended little on frequency. This phenomenon could be attributed to resistive conduction through the bulk composite including tunneling between fibers. On the other hand, at high frequencies, conductivity was proportional to frequency due to the capacitance of the matrix between the conducting particles or clusters [28].



**Fig. 7** The imaginary part ( $M''$ ) of the electric modulus versus the applied frequency for epoxy/short carbon fiber composites

The empirical Jonscher's universal law model [29] based on the aspect of the length distribution of conduction paths accessible for electric charge flow, reproduces the universal power-law dispersive ac conductivity observed in polymer networks and, generally, in a disordered matter. Power exponents near unity observed in some cases are physically acceptable within this model. A saturation high-frequency region is also predicted, in agreement with experimental results. It is generally thought, universal frequency-dependent ac conductivity of polymer composites (power-law model) takes the form:

$$\sigma_{AC} = \sigma_0 + Af^n, \quad (11)$$

where constants  $A$  and  $n$  are coefficients of values given in Table 1, and  $\sigma_0$  corresponds to the frequency independent plateau in  $\sigma$ , which is usually identified with the dc conductivity of the material. At higher frequencies, the conductivity increases as a power of frequency with power exponent  $n$  near one. Analyzing the ac conductivity by plotting  $\log [\sigma_{ac}]$  versus  $\log[f]$  is shown in Fig. 10a and b.

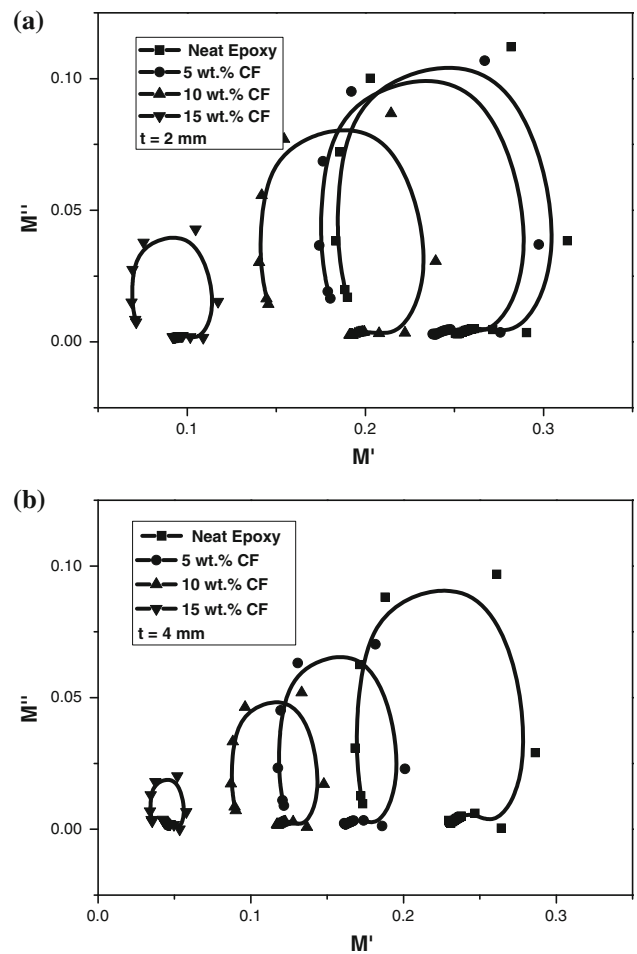


**Fig. 8** The complex plane diagram of the electric modulus

Based on this figure, it can be assumed that the equation given above under condition ( $\sigma_0$  much less than  $\sigma$ ) can be simplified to:

$$\sigma_{AC} = Af^n \quad (11')$$

It was found that the power exponents ( $n$ ) are near unity. We think that, in the present case, it is a good approximation for the approach, considering the selected frequency range from 20 Hz to 1 MHz [30, 31].

## Conclusions

In the present work, the ac electrical properties of epoxy/carbon fiber composites at different concentrations 0, 5, 10, and 15% by weight, different thicknesses 2 and 4 mm, and frequency in the range from 20 Hz to 1 MHz, the following conclusions can be obtained.

1. The dispersed CFs were randomly distributed within the epoxy matrix with some surface contacts between them.

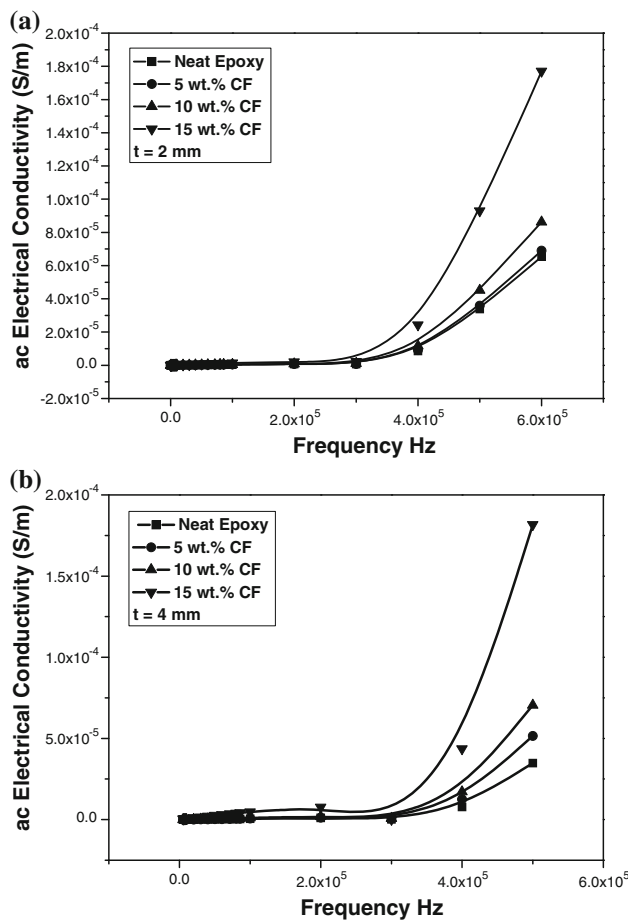


**Fig. 9** The variation of the ac electrical conductivity with the filler concentrations at different frequency

2. The endothermic step transition located was at the 140–150 °C temperature range. The glass temperature  $T_g$  was determined for the composites.
3. Impedance was found to decrease with increasing frequency, high-impedance values at low frequencies are attributed to the interfacial polarization in the matrix. The decrease in impedance indicates that the material becomes more conductive. This behavior may be attributed to the increase in the contacts of carbon fiber paths in the epoxy matrix.
4. The values of dielectric constants given for epoxy resins loaded with CFs at different concentrations increased with increasing carbon fiber content. This result could be attributed to the increase in the polarity of all blends due to the increase of carbon fiber concentration, which in turn leads to an increase in the orientation polarization and also to the presence of interfacial polarization. The increment in permittivity with the decrease of frequency reveals that the system exhibits the interfacial polarization at low frequency.

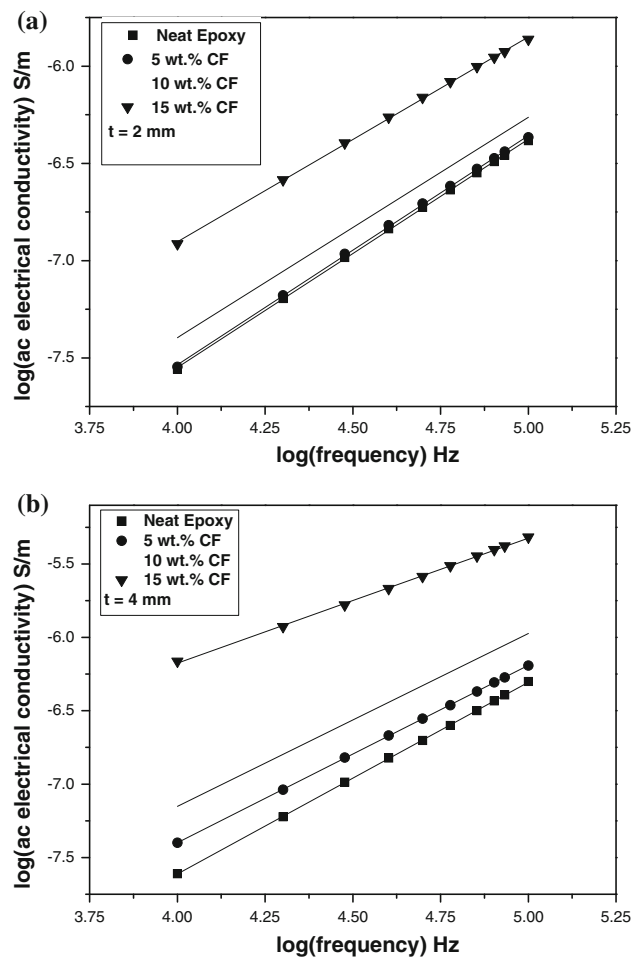


**Fig. 10** Log [ $\sigma_{\text{ac}}$ ] versus log [ $f$ ]

5. The complex plane diagram of the electric modulus displays single arcs, which prove the existence of the interfacial or MWS relaxation process. It can be regarded as the transition from resistive conduction through the conduction networks of CFs to the capacitance conduction through the capacitors in the matrix.
6. The conductivity in all compositions increases with the frequency applied. This increase means charge carriers are sufficiently free to follow the changing electric field and therefore the conductivity is frequency dependent. At higher frequencies, the conductivity increases rapidly indicating a breakdown of the dielectric behavior. When the concentration of CFs is high enough, a continuous carbon network is formed in the solid polymer matrix. As we know, the electron tunneling is the dominant transport process in carbon fiber–polymer composites.
7. The universal power-law dispersive ac conductivity observed in composites gives power exponents around unity.

**Acknowledgements** The authors would like to thank the DFG (German Research Foundation) for financial support under Schu 926 18-1, and also thanks to the Institute of Polymers and Composites at Technische Universität Hamburg-Harburg, Germany, for cooperation and technical support.

## References

1. Navin C, Deepak J (2004) Bull Mater Sci 27:227
2. Delmonte J (1990) Metal/polymer composites. Van Nostrand Reinhold, New York
3. Neelakanta PS (1995) Handbook of electromagnetic materials. CRC Press, Boca Raton
4. Surendra K, Neeti S, Ray BC (2009) J Reinf Plast Compos 28:16
5. Anupama K, Paramjit S, Jyoti I (2010) J Reinf Plast Compos 29:1038
6. Tsotra P, Friedrich K (2003) Compos A Appl Sci Manuf 34:75
7. Tse KW, Moyer CA, Arajs S (1981) Mater Sci Eng 49:41
8. Lei L, Yiping T, Haijun Z, Jianhua Z, Wenbin H (2008) J Mater Sci 43:974. doi:[10.1007/s10853-007-2089-5](https://doi.org/10.1007/s10853-007-2089-5)
9. Donnet JB, Bansal RC, Wang MJ (1990) Carbon fibers, 3rd edn. Dekker, New York
10. Park SJ, Chou MS (2000) Carbon 38:1053
11. Chand S (2000) J Mater Sci 35:1303. doi:[10.1023/A:1004780301489](https://doi.org/10.1023/A:1004780301489)
12. Rozik NN, Asaad JN, Iskander BA, Abd-El-Messieh SL (2009) J Reinf Plast Compos 28:2817
13. Teh PL, Mariatti M, Akil HM, Yeoh CK, Seetharamu KN, Wagiman AN, Beh KS (2007) Mater Lett 61:2156
14. Ellis B (1993) Chemistry and technology of epoxy resins. Chapman and Hall, London
15. El-Tantawy F, Kamada K, Ohnabe H (2002) Mater Lett 57:242
16. Achour ME, Brosseau C, Carmona F (2008) J Appl Phys 103:094103
17. Christopher J, Christopher V (2000) Compos Sci Technol 60:315
18. Xiaojun W, Chung DD (1996) Smart Mater Struct 5:796
19. Singh V, Kulkarni AR, Rama Mohan TR (2003) J Appl Polym Sci 90:3602
20. Tsangaris GM, Psarras GC, Kontopoulos AJ (1991) J Non-Cryst Solids 116:131
21. Elimat ZM, Zihlif AM, Ragosta G (2008) J Phys D Appl Phys 41:165408
22. Soares BG, Leyva ME, Barra GM, Khastgir D (2006) Eur Polym J 42(3):676
23. Abd-El-Messieh SL, Abd-El-Nour KN (2003) J Appl Polym Sci 88:1613
24. Ying X, Yuezhen B, Chiang CK, Masaru M (2007) Carbon 45:1302
25. Macedo PB, Moynihan CT, Bose R (1972) Phys Chem Glasses 13(2):171
26. Tsangaris GM, Psarras GC, Kouloumbi N (1998) J Mater Sci 33(8):2027. doi:[10.1023/A:1004398514901](https://doi.org/10.1023/A:1004398514901)
27. Ben AI, Rekik H, Kaddami H, Raihane M, Arous M, Kallel A (2009) J Electrostat 67:717
28. Psarras GC, Manolkaki E, Tsangaris GM (2002) Compos A Appl Sci Manuf 33:375
29. Jonscher AK (1983) Dielectric relaxation in solids. Chelsea Dielectric Press, London, UK
30. Prabakar K, Narayansass SK, Mangalaraj D (2002) Cryst Res Technol 37:1094
31. Ayad A, Saq'an S, Ramadin Y, Zihlif A (2006) J Thermoplast Compos Mater 19:531